

Adaptive Quadrilateral Distance Relaying Scheme for Fault Impedance Compensation

Ujjaval J. Patel* (*Assistant Professor, Vadodara Institute of Engineering, Gujarat, India*),
Nilesh G. Chothani (*Associate Professor, A.D. Patel Institute of Technology, Gujarat, India*),
Praghnes J. Bhatt (*Professor, C.S. Patel Institute of Technology, Gujarat, India*)

Abstract – Impedance reach of numerical distance relay is severely affected by Fault Resistance (R_F), Fault Inception Angle (FIA), Fault Type (FT), Fault Location (FL), Power Flow Angle (PFA) and series compensation in transmission line. This paper presents a novel standalone adaptive distance protection algorithm for detection, classification and location of fault in presence of variable fault resistance. It is based on adaptive slope tracking method to detect and classify the fault in combination with modified Fourier filter algorithm for locating the fault. To realize the effectiveness of the proposed technique, simulations are performed in PSCAD using multiple run facility & validation is carried out in MATLAB® considering wide variation in power system disturbances. Due to adaptive setting of quadrilateral characteristics in accordance with variation in fault impedance, the proposed technique is 100 % accurate for detection & classification of faults with error in fault location estimation to be within 1 %. Moreover, the proposed technique provides significant improvement in response time and estimation of fault location as compared to existing distance relaying algorithms, which are the key attributes of multi-functional numerical relay.

Keywords – Computer numerical control; Discrete Fourier transforms; Electrical fault detection; Phasor measurement; Power system faults; Power system protection.

I. INTRODUCTION

During major disturbances in power system, protection and control actions must halt power system degradation, minimize impacts and facilitate the system restoration [1]. Though, the existing protection and control actions are well designed, sometimes they fail to minimize the breakdown, which is the main cause of cascade tripping and widespread blackouts [2]. The power system protection schemes must be sensitive to unseen hidden failures, which remain undetected until the relay is exposed to certain system conditions [3].

The critical requirements for numerical distance protection are reliable and fast phasor estimation of input signals to determine correct impedance reach. An accurate apparent impedance measurement is very important because false phasor estimation might result in delayed tripping signal [3]. The accuracy and response time of any numerical distance relay depends on algorithm used for phasor estimation of input signals used in computer numerical control. Recently, many filter algorithms are available for accurate and fast phasor estimation using wavelet analysis [4]–[6]. The main issues

with these algorithms are error in estimation and delayed operation due to influence of decaying DC component. Some algorithms implement Kalman filters [7], least-square-fitting [8] and mimic filter [9] but their slower convergence speed is the critical issue. Apart from this, the time constant of the decaying DC component is unknown; if it matches with the assumed value of the time constant then only accurate phasor estimation will be performed.

An application of distance relaying scheme to compensate fault location errors due to fault resistance is presented in [10] based on Discrete Fourier Transform (DFT). It is found that the error in estimation increases up to 6.5 %, which is a major indicator of inappropriate phasor estimation. J. Linčiks et al. [11] proposed distance relaying algorithm for L-G fault on medium voltage distribution network based on digital computation for fault location estimation. Two methods are proposed, namely, improved fundamental frequency method and admittance method. The former provides an accuracy of 10 % and the latter provides an accuracy of 5 % for locating the faults, which are not sufficient during practical implementation.

Wen et al. [12] presented fast distance relaying scheme based on Equal Transfer Process of Transmission Lines (ETPTL), which implements a low pass filter for the elimination of high frequency components. However, the error in fault location estimation up to 5 % is achieved, which is not enough for accurate and fast relaying applications. Jamil et al. [13] presented Generalized Neural Network (GNN) and wavelet based approach for fault location estimation of a transmission line during wide variation of power system disturbances. The performance is compared with ANN based scheme but, the same is not validated for high resistance fault conditions. A. Yadav et al. presented a transmission line relaying scheme for fault detection and classification using wavelet transform and linear discriminant analysis [14] and an ANN based [15] fault location in TCSC compensated transmission line. However, the effect of decaying DC component and about to reach operation of the relay is not considered. Also, ANN based fault detection methods require high level of training effort for good performance especially during varying operating conditions.

* Corresponding author.

E-mail: ujjaval58@rediffmail.com

In the present era, the more efficient distance relaying algorithms are evolved by many researchers. In majority of these algorithms, phasor estimation has been performed by Fourier or wavelet transforms for generation of feature vector, which is then applied to soft computing based classifier to estimate fault context. Out of twelve discrete relaying algorithms referred in [16], only distance protection algorithm outlined in [17] and modified Fourier filter algorithm [18], respond satisfactorily and robustly to wide range of input signals. The feature vectors extracted by Discrete Wavelet Transform (DWT) are utilized by Genetic Algorithm (GA) based fault classifier in [19] and support vector machine based classifier in [20]. The main setback of the above algorithms as applied to distance protection are training and testing accuracy, determination of unknown regulation parameters and complexity for implementation. Moreover, aforesaid algorithms can be applied to the configuration of transmission for which it has been trained. It cannot be applied to other stand-alone power system network configuration without accurate training and testing. A. Sauhatset et. al. [21] presented out-of-step relay testing procedure for distance relays but the same is not validated for symmetrical fault detection during power swing involving high electrical resistance. Afterwards, U. Patel et al. [22] have outlined symmetrical fault detection during out of step condition. However, power system protection at the time of fault is not provided using adaptive distance relaying.

Compensation of Ground Distance Function (GDF) and resistive reach assessment in quadrilateral characteristics is proposed by Sorrentino [23]. This method of compensation gives the suitable results during phase impedance calculations but still needs improvement in adaptive calculation of resistive reach of relay. M. Pasand et al. [24] and A. Yadav [25] described adaptive decision logic to enhance distance protection of transmission line. However, during occurrence of high resistance faults, delayed tripping of numerical relay cannot be avoided by the said algorithms.

Many numerical distance relaying algorithms were suggested by researchers in the past for detection of High Impedance Faults (HIF). Quadrilateral relay characteristic is widely used, which incorporates more fault impedance depending on its setting compared to Mho type distance relay. If zone 1 fault involves resistance higher than the setting of quadrilateral characteristic, the relay deems this fault as of zone 2 or zone 3 and will issue delayed trip signal. A delayed tripping of circuit breaker during fault can increase stress on power system for longer time duration. The distance relay is more susceptible to under reach when HIF occurs in the third zone. This paper is mainly intended to completely eliminate the effect of any value of fault resistance by modifying the quadrilateral relay characteristic settings adaptively. Adaptive protection modifies the preferred protective response in order to make it more attuned to prevailing power system conditions. In the proposed work, quadrilateral characteristic is adaptively set to improve the response time by mitigating the adverse effect of fault resistance, DC component and pre-fault power flow condition.

II. SYSTEM MODELING

The single line diagram of a 220 kV power system network is shown in Figure 1. There are two generators (G1 and G2) connected by the first section of 120 km parallel transmission lines between Sending End Bus (SEB) and Middle End Bus (MEB) followed by the second section of 100 km single transmission line between MEB and Receiving End Bus (REB). Generators (G1 and G2) are modelled as an equivalent dynamic source representing a multi-machine system. Voltage and current signals of bus PTs at SEB and line-1 CTs are sampled at a frequency of 4 kHz (80 samples/cycle) and applied to the numerical distance relay R (Figure 1). Bergeron line model with distributed parameters is used for modeling of transmission line. The performance of numerical distance relay R is tested for all protective zones of power system network. Zone 1 covers 100 km of transmission line L_1 . Zone 2 covers remaining part of L_1 plus 50 % length of L_2 or L_3 , and zone 3 covers the remaining portion of L_2 or L_3 .

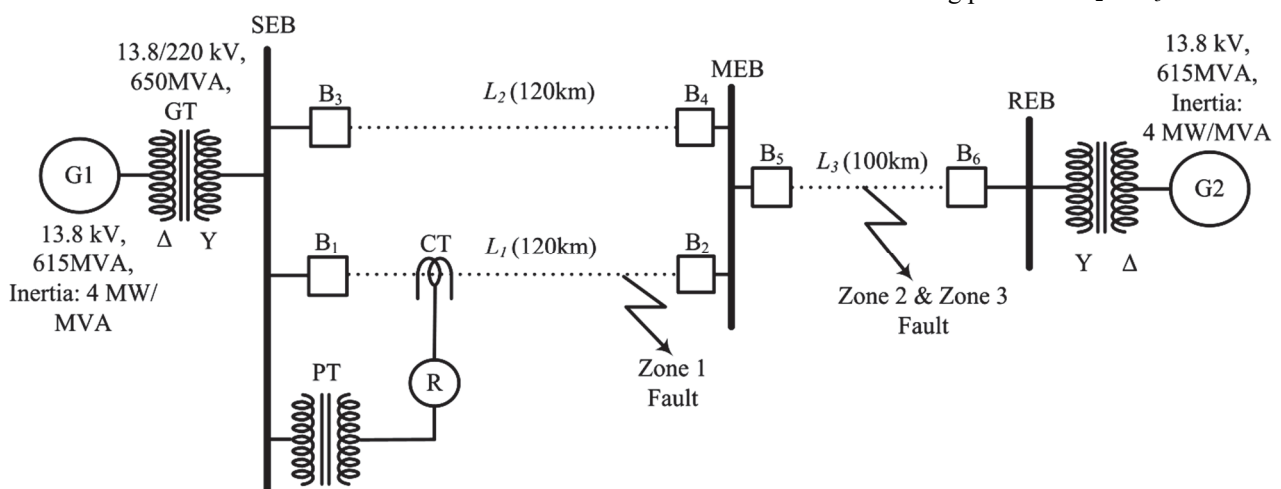


Fig. 1. Single line diagram of power system.

The proposed technique is validated for different faults such as L-G, LL, LL-G, LLL-G (10 types) at several locations in the modelled power system network to cover the effect of close-in fault, in-zone fault and out-of zone fault. Moreover, faults are simulated with different fault inception angle (0° – 315°), power flow angle (5° , 10° , 15° , 25° , 35° , 45°) and varying fault resistance (0.01Ω to 200Ω). The load in power system is varied by adjusting the variable load angle between the two generators. Large numbers of simulation cases are generated using multi-run facility available in PSCAD/EMTDC. The phasor values of voltage and current signals are successfully estimated using Modified Full Cycle Discrete Fourier Transform (MFCDFT) and applied to adaptive slope tracking algorithm for HIF detection. The factors influencing the performance of distance relays are explained in Section III followed by the proposed methodology in Section IV. The result discussion and its comparative analysis are presented in Section V.

III. FACTORS INFLUENCING PERFORMANCE OF DISTANCE RELAYS

The distance relays can mal-operate for fault context identifications because of incorrect phasor estimation and ultimately lead to delayed protective actions. The correctness of the phasor estimation depends on many parameters of the fault involved and transmission line to be protected. The detailed explanations on each of the influencing parameters are presented in this section with appropriate mathematical fundamentals.

A. Effect of DC Component

The accuracy of any distance relaying algorithm depends on proper extraction of fundamental complex phasor. However, when the fault occurs, the DC component and harmonics will be superimposed on the original phasor resulting in incorrect estimation. The most widely used phasor estimation technique is DFT, for proper extraction of fundamental component from the original phasor by separating DC component and harmonics.

The detailed discussion on the same is as follows: Let $x(t)$ be the sinusoidal time varying signal, which is to be analyzed. $X(k)$ is the discrete time signal derived from $x(t)$ by sampling it with sampling frequency f_s . Assuming that the continuous time signal containing a DC offset A_0 , it can be represented by the equation:

$$x(t) = A_0 + \sum_{n=1}^N A_n \cos(n\omega t + \theta_n) \quad (1)$$

Its discrete time signal can be obtained by putting $t = k\Delta T$.

$$X(k) = A_0 + \sum_{n=1}^N A_n \cos(n\omega k\Delta T + \theta_n) \quad (2)$$

where, T is fundamental cycle time; N is number of sample in window of a full cycle; $\Delta T =$ sampling time $= T / N$; n indicates frequency component contained in complex phasor $x(t)$, $n = 0$ indicates fundamental frequency component of the complex phasor, k is the sample number and $X(k)$ indicates complex phasor of the k^{th} sample.

Now, $\omega = 2\pi f = \frac{2\pi}{T} = \frac{2\pi}{N\Delta T}$.

Putting this value of ω in eq.(2), we get

$$X(k) = A_0 + \sum_{n=1}^N A_n \cos\left(\frac{2\pi kn}{N} + \theta_n\right). \quad (3)$$

Eq.(3) represents DFT of an input analog signal $x(t)$. The effect of DC component and error in phasor estimation due to variation in FIA are discussed in the next section.

B. Effect of Fault Inception Angle

The magnitude of DC component depends on the fault inception angle α as given by the eq. (4):

$$A_0 = A_n \sin(\theta - \alpha) e^{-\frac{t}{\tau}}, \quad (4)$$

where, A_n indicates maximum magnitude of the signal, $\theta =$ phase of the signal, $\alpha =$ fault inception angle, and τ is the time constant of the system. By using eq.(3) of full cycle DFT, phasor estimation of voltage and current waveform can be performed for the fault analysis and impedance can be calculated. The DC component will be maximum when the FIA is 0° and minimum when the FIA is 90° . When FIA is 0° due to the error in the phasor estimation, relay can mal-operate. If the impedance locus is lying near the boundary of the characteristics of the relay, it can result in under reaching problem. So, these limitations can be easily overcome by MFCDFT, as discussed in Section IV A, resulting in accurate phasor estimation during extreme fault conditions. The comparative analysis for removal of the effect of decaying DC component and FIA is presented in Section V A.

C. Effect of Load Encroachment

In order to make the zone adoption technique immune to load encroachments, authors have analyzed the proposed technique for various loading scenarios by varying the power flow angle from 5° to 45° as outlined in Section II. Heavy loads in the system can be mistaken as faults occurring in zone 3 as shown in Figure 2. Such conditions lead to overreaching problems.

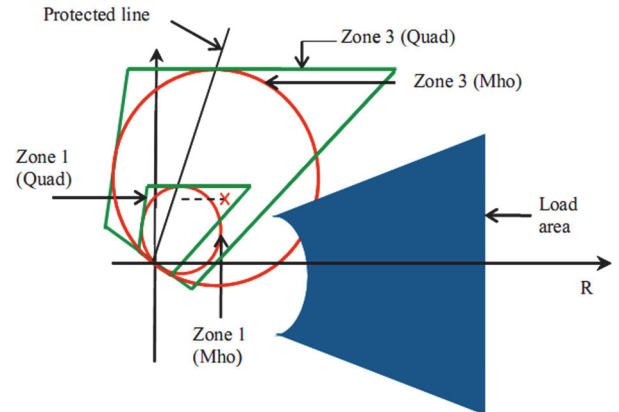


Fig. 2. Comparison between Mho and quadrilateral settings for load encroachment problems.

The incorrect operation of distance relays due to large load encroachments was the root cause of several historical blackouts in India and the USA. In the past, when the electromechanical relays were used, circular Mho characteristic was the only possible choice. But nowadays, variety of relay characteristics can be realized with the numerical relays. Figure 2 shows a quadrilateral relay with the same reach settings as that of relay with Mho characteristics. It can be observed that Mho settings are more immune to heavy loads, which ultimately results in mal-operation. However

with the use of quadrilateral settings, trip signal is blocked during heavy load conditions. Hence, in order to make the relay more sensitive to high resistance faults and less sensitive to heavy loads, quadrilateral characteristic is employed in the present work of developed scheme. Moreover, it was observed that for very heavy loading conditions the load impedance can encroach even quadrilateral settings as well in zone 3. In order to prevent the same, zero sequence components of fault currents can be used for proper discrimination as discussed in Section IV B.

D. Influence of Load Flow and Fault Resistance

The magnitude of DC component depends on the fault inception angle α as given by the eq. (4). Figure 3 shows simple two-terminal transmission line between two buses. If fault occurs in the middle of the transmission line (between bus A and B), the impedance seen by the relay can be given by

$$Z_{\text{seen}} = d \cdot Z_L + R_F \left(1 + \frac{I_B}{I_A}\right) \quad (5)$$

where Z_L is the unit line impedance, and d indicates fault location. Also, $I_F = \text{fault current} = I_A + I_B$.

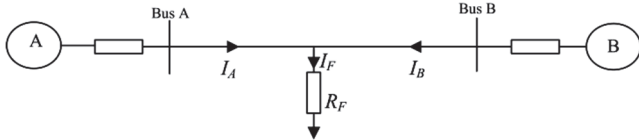


Fig. 3. High resistance fault in transmission line

When HIF occurs, not only R_F changes but magnitude and phase of fault current will also change depending on pre-fault power flow conditions. Thus, due to pre-fault condition for L-G fault, if Z_{seen} is higher than the set value in the distance relay then under reach can happen. Hence, there is a need of adaptive distance relay, which can change its characteristics according to the magnitude of fault resistance dynamically during real time operations. The detailed discussion on adaptive slope tracking method to eliminate the influence of power flow and fault resistance is outlined in Section IV D.

IV. PROPOSED METHODOLOGY

Figure 4 represents the proposed algorithm, which consists of three main steps:

- A) phasor estimation using MFCDFT;
- B) impedance reach calculation using slope tracking method;
- C) adaptive setting of quadrilateral characteristic for determination of relay decisions.

A. Proposed Phasor Estimation Technique

In conventional numerical relay, DFT is used for phasor estimation to extract fundamental component from the original complex phasor. The main limitation of DFT algorithm is inaccurate removal of decaying DC component and higher order harmonics from the original complex phasors. Hence, to overcome the said error for accurate phasor estimation during extreme fault conditions, MFCDFT is realized. The fault and abnormal conditions are discriminated with the help of fault detection algorithm based on MFCDFT followed by low pass Butterworth filter to remove harmonic and aliasing effects. A signal compensation for accurate phasor estimation is

employed in account of three more samples.

During the faulty condition, exponentially DC component will be superimposed on the fundamental component, having magnitude D and time constant τ . It can be represented by $X_{DC} = D e^{-\frac{t}{\tau}}$. The output of low pass filter contains additional DC component having magnitude, say D_1 , and time constant $\tau_1 > 0$. When the fault occurs, the DC component will be superimposed on fundamental phasor, which results in incorrect phasor estimation. The real part $X_{r1}(k)$ and imaginary part $X_{i1}(k)$ for the fundamental complex phasor at any k -th sample can be obtained using MFCDFT as

$$X_{r1}(k) = X_r(k) - \frac{2}{N} \sum_{n=k-N+1}^k \left(D e^{-\frac{n\Delta T}{\tau}} + D_1 e^{-\frac{n\Delta T}{\tau_1}} \right) \cos\left(\frac{2\pi n}{N}\right); \quad (6)$$

$$X_{i1}(k) = X_i(k) + \frac{2}{N} \sum_{n=k-N+1}^k \left(D e^{-\frac{n\Delta T}{\tau}} + D_1 e^{-\frac{n\Delta T}{\tau_1}} \right) \sin\left(\frac{2\pi n}{N}\right), \quad (7)$$

Where k is in-progress sample number, ΔT is sampling time, f_0 is fundamental frequency, D is constant of DC component, D_1 is constant of digital filter, N is number of samples/cycles, τ is time constant of the line to be protected, n varies for N number of samples of the last cycle, and τ_1 is time constant of digital filter.

In the proposed work, in order to estimate all the voltages and currents simultaneously at any instance, the phasor (real and imaginary part) for any j -th signal at k -th instance can be given by,

$$X_{r1}(j, k) = X_r(j, k) - \frac{2}{N} \sum_{n=k-N+1}^k \left(D(j) e^{-\frac{n\Delta T}{\tau(j)}} + D_1(j) e^{-\frac{n\Delta T}{\tau_1}} \right) \cos\left(\frac{2\pi n}{N}\right), \quad (8)$$

$$X_{i1}(j, k) = X_i(j, k) + \frac{2}{N} \sum_{n=k-N+1}^k \left(D(j) e^{-\frac{n\Delta T}{\tau(j)}} + D_1(j) e^{-\frac{n\Delta T}{\tau_1}} \right) \sin\left(\frac{2\pi n}{N}\right). \quad (9)$$

The unknown parameters D and D_1 are calculated by estimating phasors from eq. (8) and (9) for the next three samples and then by taking their ratio. The magnitude and phase angle for one complete cycle are calculated by using the equation

$$|X(j, k)| = \sqrt{(X_{r1}(j, k))^2 + (X_{i1}(j, k))^2}, \quad (10)$$

$$\angle(X(j, k)) = \tan^{-1}\left(\frac{X_{i1}(j, k)}{X_{r1}(j, k)}\right). \quad (11)$$

Those equations give magnitude and phase angle of j -th signal at k -th instance. Also eq.(10) gives maximum magnitude and eq.(11) gives phase angle, including the effect of three more samples and hence it can result inaccurate phasor estimation. To correct it, RMS value of $X(j, k)$ is given by

$$M_j = \frac{|X(j, k)|}{\sqrt{2}}. \quad (12)$$

Here, cosine Fourier transform is performed to estimate the phasor magnitude, hence there will be phase displacement of 90° and delay of three samples is also to be taken into account. To compensate for the change in signal parameters, the actual phase angle of the fundamental complex phasor is given by

$$\theta_j = \angle(X(j, k)) - \left(90^\circ + \left(3 \frac{360^\circ}{N}\right)\right). \quad (13)$$

Eq.(12) and (13) give the RMS value and phase angle respectively, for fundamental complex phasor after removal of all the harmonics and decaying DC component, hence they can be used for further calculation of impedance/distance.

B. Impedance Reach Determination

Once accurate phasors for bus voltages V_a, V_b, V_c and line currents I_a, I_b, I_c are obtained by MFCDFDT, sequence components are calculated from the phasor voltages and currents using the equation

$$\begin{bmatrix} V_1 \\ V_2 \\ V_0 \end{bmatrix} = \frac{1}{3} \begin{bmatrix} 1 & a & a^2 \\ 1 & a^2 & a \\ 1 & 1 & 1 \end{bmatrix} \begin{bmatrix} V_a \\ V_b \\ V_c \end{bmatrix} \text{ and } \begin{bmatrix} I_1 \\ I_2 \\ I_0 \end{bmatrix} = \frac{1}{3} \begin{bmatrix} 1 & a & a^2 \\ 1 & a^2 & a \\ 1 & 1 & 1 \end{bmatrix} \begin{bmatrix} I_a \\ I_b \\ I_c \end{bmatrix}, \quad (14)$$

where $a = -0.5 + 0.866i$. Normally, phase impedances referred to ground fault can be calculated using the equation

$$Z_p = \frac{V_p}{I_p + K_0 I_0} \quad (15)$$

In conventional relay, K_0 is assumed between 1.5 and 3.5 i.e. a constant value, which depends on the fault resistance, tower footing resistance and soil resistivity. A comparison of five different methods for calculating the ground distance function (GDF) is presented in [23] and adaptive calculation of GDF is proposed. Thus, instead of taking it as a constant value for finding the value of Z_p , it can be calculated as follows:

$$K_0 = \frac{Z_{L0} - Z_{L+}}{3Z_{L+}}, \quad (16)$$

where Z_{L+} = positive sequence impedance = $\frac{V_1}{I_1}$ and Z_{L0} = zero sequence impedance = $\frac{V_0}{I_0}$.

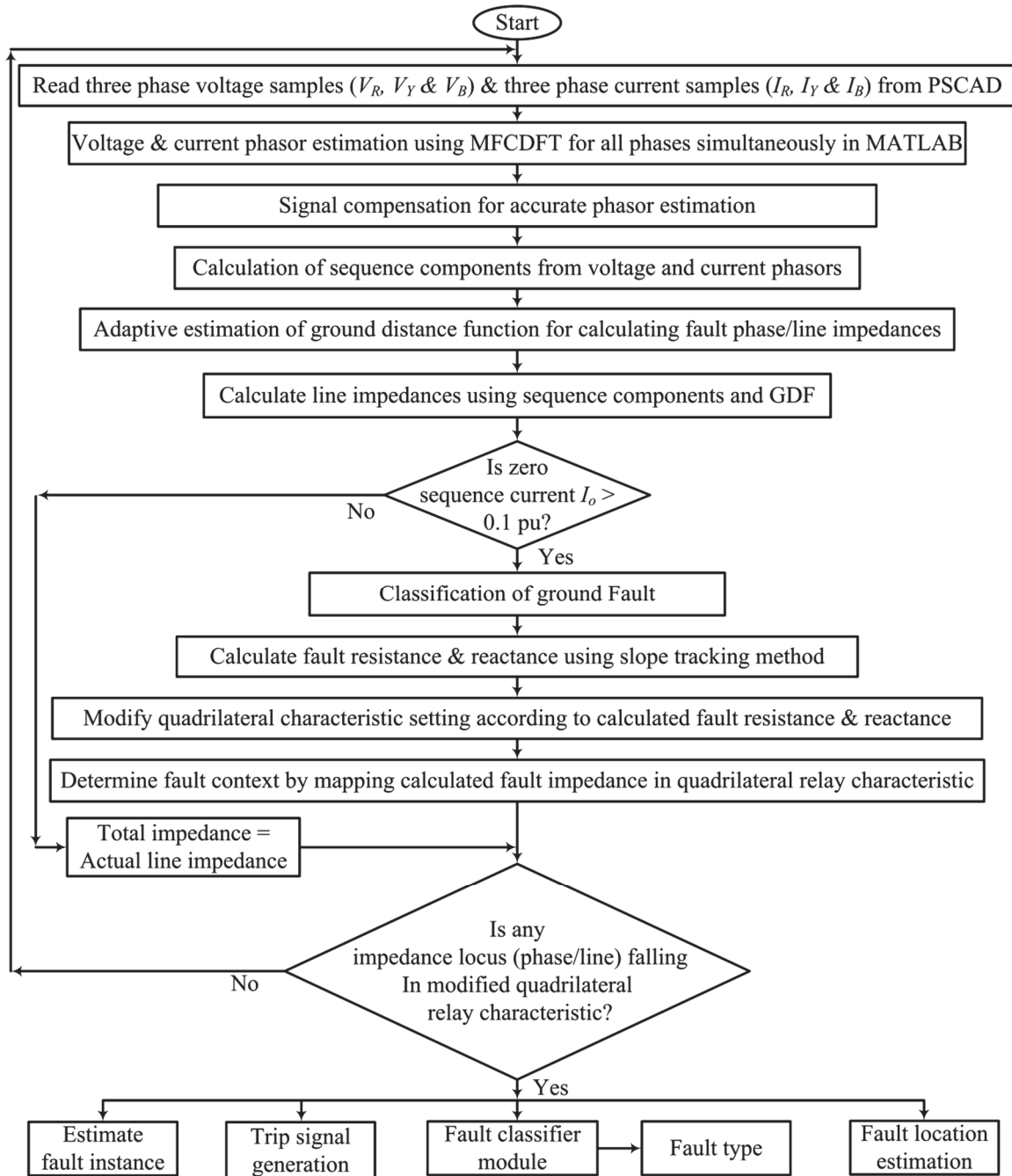


Fig. 4. Proposed methodology for transmission line protection.

The developed scheme is also examined for the load encroachment problems of proper discrimination between heavy load and fault scenarios. In order to prevent the same, zero sequence components of fault currents have been used for proper discrimination. Whenever zero sequence current I_0 is more than 0.1 pu of maximum load current (as shown in Figure 4), HIF is detected. During HIF, impedance reach has been determined from estimated sequence components and GDF. The calculated fault impedance comprises line impedance and fault resistance. In case of high resistance ground fault, the estimated fault impedance trajectory can fall outside the tripping region of the distance relay and result in delayed tripping or under reach operation of the relay. This can be overcome by estimating fault resistance using slope tracking method as discussed in Section IV D. As one cannot modify the fault impedance seen by the relay, but it is very easy to modify the characteristics of relay itself. Hence, fault resistance estimated using slope tracking method is further used to modify the relay settings for taking protective actions. During load encroachments, the zero sequence component remains within 0.1 pu of maximum load currents, which ultimately blocks the trip signal. Hence, even though the impedance locus falls inside the quadrilateral characteristics, the proposed methodology blocks the trip signal indicating stability and reliability of the protective scheme.

The value of line impedances referred to phase fault can be calculated using the following equations:

$$Z_{ab} = \frac{V_a - V_b}{I_a - I_b}; \quad Z_{bc} = \frac{V_b - V_c}{I_b - I_c}; \quad Z_{ca} = \frac{V_c - V_a}{I_c - I_a}. \quad (17)$$

If any of the complex phasors of phase impedances or line impedances falls within quadrilateral characteristic, then trip signal is generated. From the knowledge of phase or line impedance locus entering into the trip region, type of fault generated in the power system can be determined. The operating time can be calculated by considering the sample number as time stamp using the following equation:

$$\text{Fault time} = \frac{(K \cdot \Delta T)}{f_0}, \quad (18)$$

Where K is sample number, ΔT is sampling time, and f_0 is fundamental frequency. In the next sections, setting calculations of quadrilateral relay is explained in detail followed by slope tracking method for adaptive distance protection.

C. Relay Settings for Protection Zones

Proper understanding of transmission line parameters and protection issues forms the basis for arriving at the right relay settings [26]. This section contains the settings of quadrilateral relay by using the line and system parameters for detection of high resistance fault for all zones followed by adaptive slope tracking method to detect and classify the faults. Backup protection is provided in distance protection using stepped distance characteristics.

Zone 1 or the high-speed zone is set to trip without any intentional time delay and provides primary protection for the line section to be protected, which can be adjusted to reach 80–90 % of the line length. Figure 5 shows setting of quadrilateral relay for different zone of protection. Zone 1

relay setting is done for initial 100 km of line L_1 for the system modeling shown in Section II. According to the guidelines published by subcommittee on relay/protection task force for power system analysis under contingency [26] for detecting the high resistance fault, minimum 15 Ω arc resistance should be considered during setting of relay. In order to incorporate the effects of close-in fault, Negative Restraint Angle (NRA) is set to 115° (line AB) and Directional Angle (DA) for distance protection is adjusted to -15° (line AD). As line impedance considered is $(0.0297 + j0.332) \Omega/\text{km}$, hence the total line impedance for 100 km will be $(2.97 + j33.2) \Omega$ for zone 1 protection. Here, considering X/R ratio of 11 as per guidelines in [26], line impedance can be rounded to $(3 + j33) \Omega$. As fault current is limited by source impedance, line impedance and fault impedance; to calculate total reactance, source impedance $(0.871 + j9.96) \Omega$ must be considered and hence maximum reactance during the fault will be 43 Ω and hence line BC is drawn at a height of 43 units from the origin A. To incorporate fault resistance (R_F) of 15 Ω with line resistance (R_L) of 3 Ω , total impedance will be $Z_T = (18 + j43) \Omega$, which yields line angle $\phi = \tan^{-1}\left(\frac{43}{18}\right) = 67.28^\circ$. Hence, considering $AF = 18$, line CD is drawn at an angle of ϕ with x -axis.

Zone 2 is used to provide high-speed protection for the remainder of the line and also serves as backup protection for 50 % section of an adjoining line. The second-zone relays have to be time delayed to coordinate with relays at the remote bus with typical time delays of around 0.1–0.5 s. Lines AB and AD are drawn in exactly the same manner as that of zone 1. Zone 2 covers in total 170 km from the relay location with total line resistance of 5 Ω . By considering X/R ratio of 11, the line reactance will be 55 Ω . By incorporating fault resistance and source impedance, total line impedance for zone 2 will become $(20 + j65) \Omega$. Hence, PQ is drawn at a height of 65 units from the origin A and considering $AG = 20$, line QJ is drawn at the line angle of ϕ with x -axis.

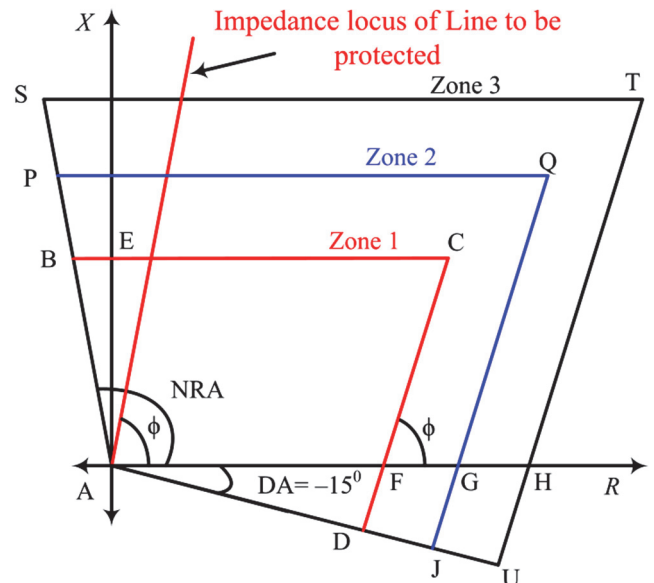


Fig. 5. Stepped distance quadrilateral characteristic for all zones.

The third zone, designated as zone 3, is used to provide remote backup to the first and second zone of an adjacent line

sections when a relay or breaker fails to clear the fault locally. The usual practice is to extend its reach beyond the end of the largest adjoining line section or more than double the line section to be protected. The third-zone operation is usually delayed by about 0.3–2.0 s. The third-zone reach setting is a more complex problem. It has been observed that the zone 3 unit trips due to load encroachment problems and thereby leads to the cascade tripping of the power system. The third-zone setting must be blocked during extreme loading conditions. In the proposed work, this blocking is achieved by monitoring the zero sequence component of fault current. The third zone relay setting is done for total 220 km from the relay location. By considering fault resistance (15 Ω) and source impedance (0.871 + j9.96) Ω, total impedance will become (22 + j87) Ω. Hence, line ST is drawn at a height of 87 units from the origin A. Further considering AH = 22, line TU is drawn at line angle of ϕ with x-axis (Figure 5). It results in complete quadrilateral characteristic considering close-in fault with directional sensitivity for all zones of protection.

D. Adaptive Slope Tracking Method

Figure 6 shows impedance trajectory $Z_T = (R_T + jX_T)$ during high impedance fault for different power flow conditions. It is observed that during solid L-G fault ($R_F = 0 \Omega$), the apparent impedance Z_T is located along the segment described by the line impedance Z_{Line} , while varying R_F without power transfer between SEB & MEB represents a straight line that increases depending on resistive reach as shown in Figure 6(a). However, when both R_F and pre-fault power conditions are considered, the locus of the apparent impedance Z_T follows a slight curvature like downwards concave when exporting power from SEB (Figure 6(b)) and upwards concave when importing power conditions (Figure 6(c)). Exporting power from SEB results decrease of apparent impedance and importing power results increase in apparent impedance seen by the relay. It can ultimately lead to mal-coordination between distance protection zones. As shown in Figure 6(d), Z_a indicates fault impedance without considering high resistance fault.

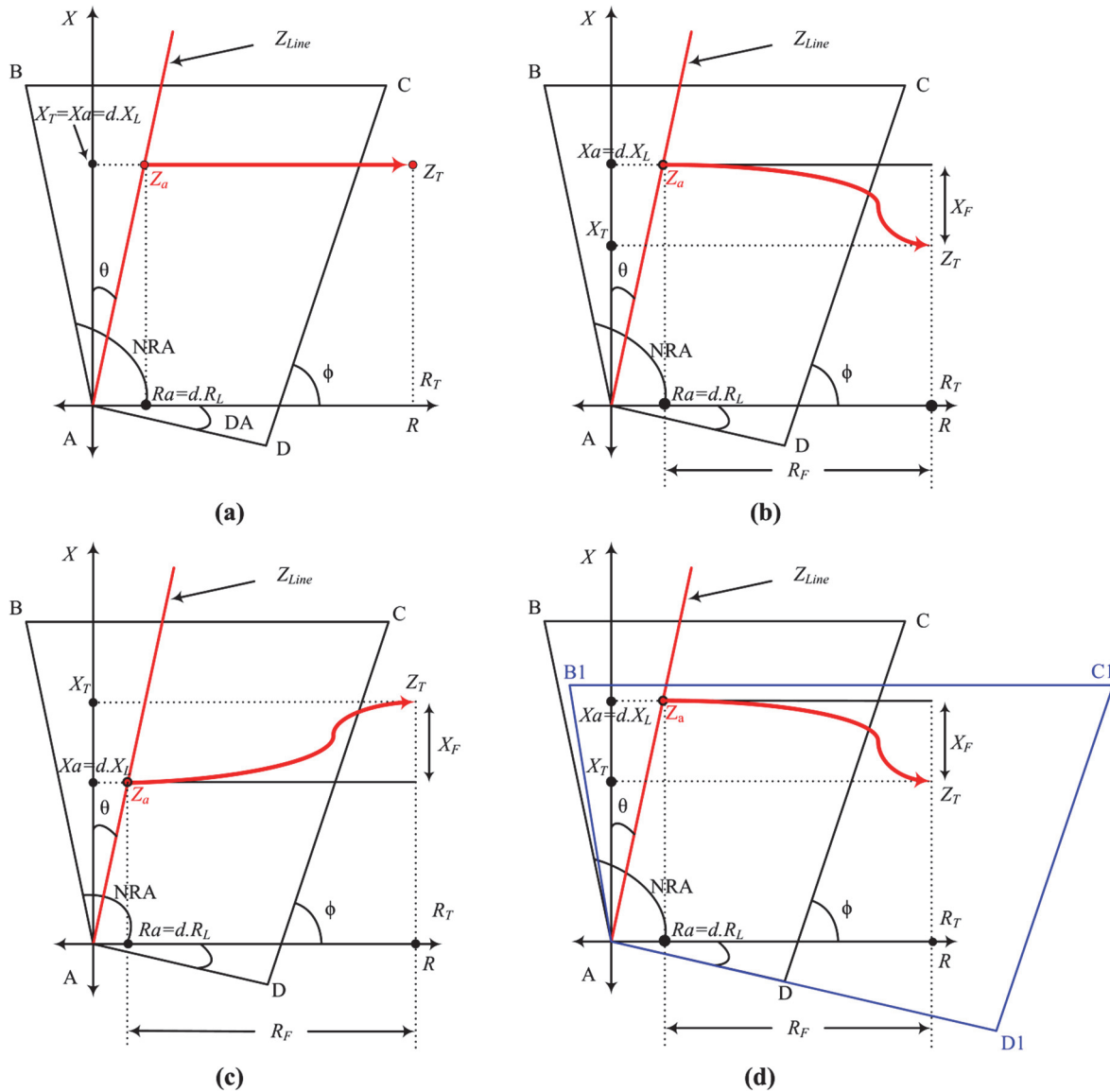


Fig. 6. Impedance trajectory Z_T during variable fault resistance R_F for different power flow conditions between SEB & MEB: (a) no power transfer; (b) exporting power flow; (c) importing power flow; and (d) adaptive characteristic during variable power flow

During solid L-G fault, due to absence of resistance in faulty path, the quadrilateral relay will easily detect the fault. Whereas during high resistance fault, the fault impedance locus will move out of the quadrilateral characteristic and result in mal-operation of the relay. In order to prevent such breakdown of the relay during the high resistance fault, line impedance locus can be traced by considering zero sequence component of the fault current and X/R ratio of transmission line. In normal conditions, zero sequence component of the fault current will be negligible and when ground fault occurs, it will rise abruptly. Here, in this investigation, a threshold value of 0.1 pu of maximum load current is considered for zero sequence current. If zero sequence current is greater than this threshold value, it indicates that ground fault has occurred. The power flow will always be exported when the fault occurs in forward direction of the relay.

During high resistance fault, due to change in system parameters the reactance seen by the relay reduces slightly. The actual phase impedance without involving fault resistance and adaptive setting of quadrilateral characteristic as shown in Figure 6(d) are done as follows.

1. Total fault impedance is given by $Z_T = R_T + jX_T$.
2. Fault resistance can be narrated from the knowledge of ground distance function (GDF) K_0 , absolute value of total impedance Z_T (Z_{abs}), and X/R ratio (XBR) of transmission line to be protected.

$$R_F = \frac{R_T \cdot XBR + K_0 X_T - (1 + K_0) Z_{abs}}{K_0 XBR} \quad (19)$$

3. Actual line resistance can be traced to $R_a = R_T - R_F$.
4. Actual line reactance can be calculated by $X_a = R_a \cdot XBR$.
5. Change in fault reactance can be traced to $X_F = X_T - X_a$.
6. Total actual line impedance $Z_a = R_a + jX_a$.
7. Absolute value of actual impedance $Z_{am} = \text{abs}(Z_a)$.
8. Absolute magnitude of unit impedance $Z_u = \text{abs}(Z_{pu})$.
9. Fault location can be derived as ratio of Z_{am} to Z_u .
10. Error in estimation of fault location can be given by

$$\% \text{ Error} = \frac{\text{Estimated Location} - \text{Actual Location}}{\text{Actual Location}} \cdot 100 \% \quad (20)$$

Settings of quadrilateral characteristics can be modified after calculating the magnitudes of R_F and X_F with the vertices of A, B1, C1, D1 as shown in Figure 6(d). The fault resistance R_F and fault reactance X_F can be applied as correction factors in coordinates of C1 and D1. In order to sense high resistance close-in faults properly, the correction factor of only X_F is applied to the coordinates of B1, which also maintains directional sensitivity of the relay. Thus, adaptive settings of quadrilateral characteristics depend on fault impedance, power flow conditions and GDF.

Estimated fault impedance locus is mapped in impedance plane of relay and if it falls within the characteristics, then the proposed numerical relaying technique issues the trip signal. Moreover, the proposed technique can also calculate fault instance by considering sample number as its time stamp. Fault classifier module is also designed to identify the type of fault occurred in power system. In order to show the effectiveness of the proposed algorithm, the results are compared with existing methods, which are implemented with the same system configuration and relay characteristics as outlined in the next section.

V. VALIDATION OF THE PROPOSED TECHNIQUE

A. Results of Phasor Estimation

The results of phasor estimation by realizing algorithms of DFT and proposed MFCDFT as mentioned in Section IV are shown in Figure 7. The results are obtained by simulating the system modeling outlined in Section II in PSCAD software for L-G fault applied at 0.1 s (400 samples). For phasor estimation at any k -th sample, pre fault 80 samples and post fault 3 samples are considered. Thus, a sliding window of 83 samples is used for phasor estimation of each sample. For the waveform shown in Figure 7, the fault is applied at k -th sample (400) and if it is detected on $k + \Delta n$ sample (453), then $\Delta n = 53$ is the number of samples required to detect the fault (fault detection time = 13.25 ms). The results indicate that the proposed technique performs phasor estimation of faulted current in a better manner as compared to conventional DFT by removing the effect of DC component and FIA. Filtering and signal compensation in magnitude and phase impedance gives improved results for each type of fault for various power system disturbances.

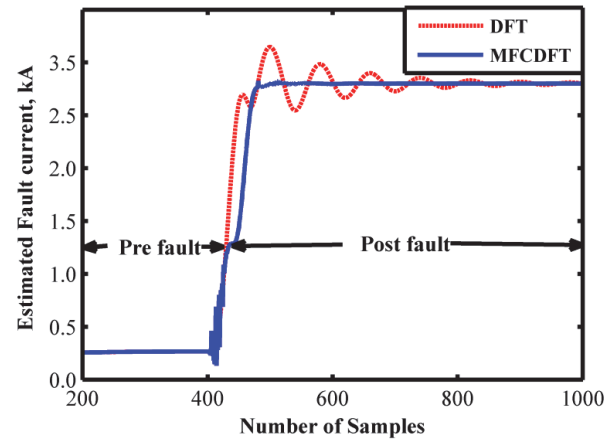


Fig. 7. Phasor estimation for fault current using DFT and MFCDFT during L-G fault applied at 0.1 s (400 samples) with FIA = 0°.

B. Performance Evaluation of the Proposed Algorithm

In order to validate the performance and reach setting of the proposed numerical relaying technique, the results are obtained by simulating different kind of faults with varying power system operating conditions as outlined in Section II. Table I shows the performance of the proposed numerical algorithm in terms of operating time for close-in faults, boundary location faults and high resistance faults simulated in all three zones during different power system disturbances.

The obtained results are compared with the existing methods based on conventional DFT, phase comparison principle [4], wavelet transform and Linear Discriminant Analysis (LDA) [14] and also Adaptive Neuro Fuzzy Inference System (ANFIS) [24] as shown in Table I.

Fault classifier module is designed to identify the type of fault occurs depending on the type of impedance locus enters into the trip region of characteristic. In fault classifier, six separate impedance modules are designed, each for individual phase (A, B and C) and for line (AB, BC and CA). The output signals TripA, TripB and TripC are for phase modules and TripAB, TripBC and TripCA are for line modules, respectively. The output of fault classifier module is shown in Table I.

TABLE I
COMPARISON OF PROPOSED TECHNIQUE WITH EXISTING SCHEME FOR VARIATION IN FAULT CONTEXT

Case No.	Fault Applied	Fault Location d , km	δ , °	FIA, °	R_f , Ω	Operation time, ms					Estimated R_f , Ω	Fault Classified	Estimated Fault Location d' , km	% Error = $\frac{d-d'}{d} \cdot 100$
						Conv. DFT	Proposed technique	Phase Comp. [4]	Wavelet & LDA [14]	ANFIS [24]				
Close-in faults														
1	A-G	5	-5	0	0.01	5.20	5.30	5.6	13	9.23	0.70	A-G	5.031	0.62
2	A-G			90	10	4.50	4.52	7.6	14	12.01	9.81	A-G	5.038	0.76
3	A-G			45	20	NOP	4.21	3.2	18	-	19.70	A-G	5.037	0.74
4	A-G		-15	0	0.01	5.40	5.31	5.8	12	9.92	0.68	A-G	5.026	0.52
5	B-G			90	10	4.70	4.54	7.6	15	12.01	9.75	B-G	5.024	0.48
6	C-G			45	20	NOP	4.21	3.4	18	-	19.65	C-G	5.040	0.80
7	A-G	10	-5	0	0.01	5.18	5.51	5.6	8	9.23	0.67	A-G	10.065	0.65
8	A-G			90	10	4.00	4.83	7.6	16	10.61	9.82	A-G	10.064	0.64
9	A-G			45	20	NOP	4.49	3.2	18	20.14	19.80	A-G	10.061	0.61
10	A-G		-15	0	0.01	5.82	5.53	5.8	9	10.62	0.65	A-G	10.068	0.68
11	A-G			90	10	5.94	4.82	7.6	16	11.31	9.75	A-G	10.066	0.66
12	A-G			45	20	6.01	4.49	3.4	18	20.34	19.65	A-G	10.065	0.65
Faults in zone 1														
13	A-G	30	-5	0	0.01	17.1	6.20	12.4	9	14.22	0.55	A-G	30.192	0.64
14	C-G		-10	0	20	NOP	11.50	13.0	18	21.80	19.14	C-G	30.205	0.68
15	A-G		-5	90	40	NOP	11.90	14.4	20	22.80	38.92	A-G	30.219	0.73
16	AB-G	30	-5	0	0.01	5.8	4.12	-	10	21.03	0.60	AB-G	30.127	0.42
17	A-G	50	-5	90	0.01	12.8	12.50	11.6	15	15.47	0.62	A-G	50.436	0.87
18	B-G		-10	0	20	NOP	12.60	15.2	18	22.41	20.23	B-G	50.441	0.89
19	C-G		-15	90	40	NOP	13.90	18.0	20	23.70	40.91	C-G	50.452	0.90
20	BC-G	50	-5	0	0.01	11.6	9.00	-	11	22.20	0.59	BC-G	50.384	0.77
21	A-G	65	-5	0	0.01	14.6	14.30	16.4	16	15.80	0.73	A-G	65.170	0.26
22	A-G	65	-10	0	20	NOP	15.50	22.0	18	-	20.46	A-G	65.122	0.19
23	A-G	65	-15	90	50	NOP	15.80	NOP	19	200	50.60	A-G	65.513	0.79
24	AB-G	65	-5	0	0.01	12.6	11.20	-	12	23.81	0.42	AB-G	65.324	0.50
25	ABC-G	65	-5	0	0.01	10.7	10.00	-	10	22.41	0.44	ABC-G	65.290	0.45
26	A-G	90	-5	0	0.01	18.0	17.30	23.0	17	19.64	0.94	A-G	90.501	0.56
27	A-G	90	-10	0	20	NOP	18.50	26.0	18	23.81	20.67	A-G	90.712	0.79
28	A-G	99	-15	90	50	NOP	19.60	NOP	NOP	200	50.75	A-G	99.614	0.61
29	CA-G	99	-5	0	0.01	14.5	13.10	-	13	22.41	0.57	CA-G	99.523	0.52
Faults in zone 2 & zone 3														
30	A-G	110	-5	0	0.01	-	214.50	NOP	NOP	23.12	1.22	A-G	110.570	0.52
31	B-G	150	-5	0	0.01	-	217.30	NOP	NOP	-	1.70	B-G	150.960	0.64
32	C-G	150	-5	0	20	-	219.20	NOP	NOP	-	21.9	C-G	151.150	0.76
33	A-G	180	-5	0	20	-	421.20	NOP	NOP	-	23.4	A-G	181.770	0.98
34	B-G	200	-5	0	0.01	-	421.10	NOP	NOP	-	2.31	B-G	201.810	0.90

Figures 8(a), 8(c), and 8(e) illustrate estimated impedance trajectories during low resistance L-G fault and Figures 8(b), 8(d), and 8(f) indicate high resistance L-G fault simulated at different location on line considered between SEB and MEB. It can be observed impedance locus at the time of fault falls outside the quadrilateral characteristics of the normal relays. Whereas, the proposed adaptive numerical relaying scheme effectively modifies its characteristics only at the time of fault and generates the trip signal to actuate the circuit breaker. It indicates efficacy of the proposed methodology.

The waveforms of phase voltages, line currents, fault applied and trip signals during fault resistances of 0.01 Ω and 20 Ω are shown in Figures 9 and 10 for Case 17 and 18 of Table I. The effect of DC component will be profound during the low fault resistance and vanish during the high fault resistance, which can be observed from Figures 9(b) and 10(b). The adaptive setting of the numerical relay is highly effective for the protection scheme under consideration.

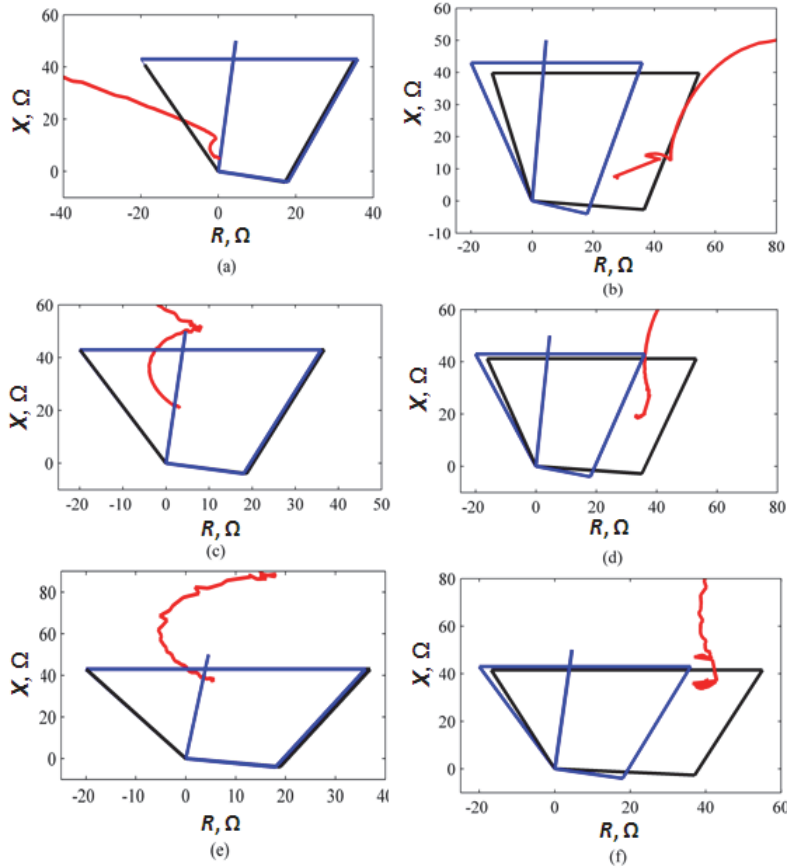


Fig. 8. Fault impedance trajectory during (a) Case 1, (b) Case 3, (c) Case 17, (d) Case 18, (e) Case 26, (f) Case 27 of Table I.

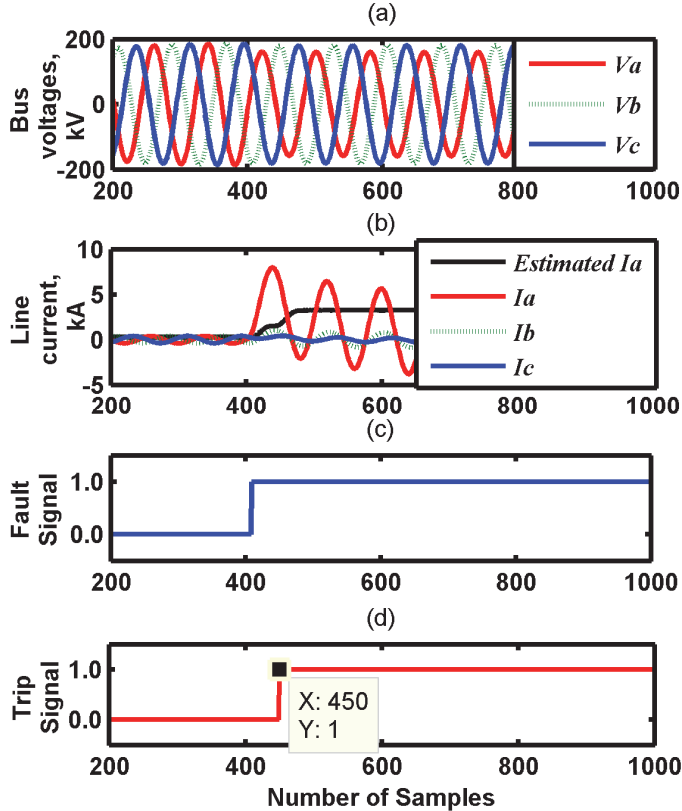


Fig. 9. (a) Bus voltages, (b) line currents and estimated value of fault current, (c) fault signal, and (d) trip signal during L-G fault applied at 50 km at 0.1 s with $R_f = 0.01 \Omega$ and $FIA = 0^\circ$.

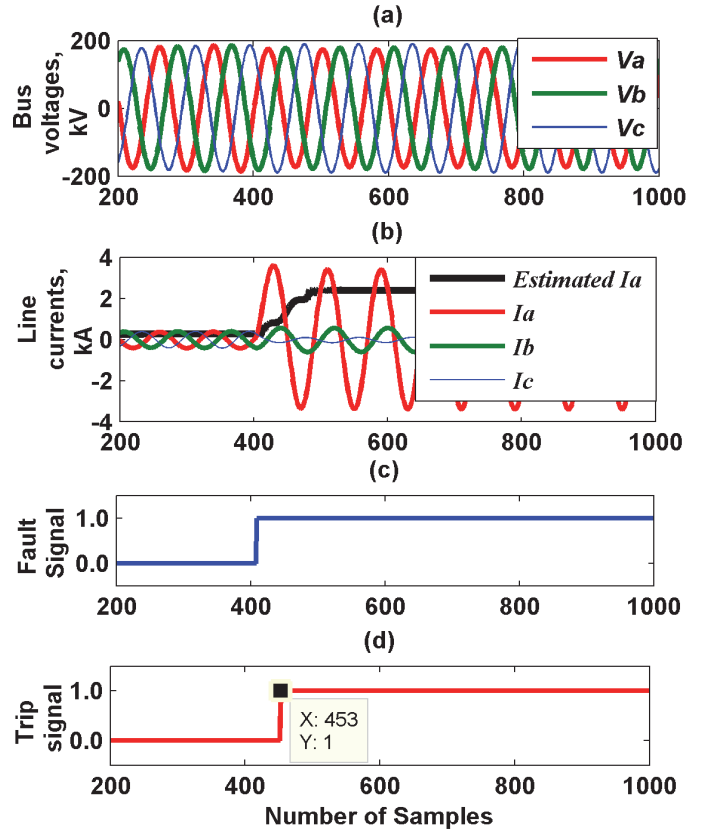


Fig. 10. (a) Bus voltages, (b) line currents and estimated value of fault current (c) Fault Signal and (d) Trip Signal during L-G fault applied at 50 km at 0.1 s with $R_f = 20 \Omega$ and $FIA = 0^\circ$.

From the comparative results demonstrated above, sound features of the proposed technique can be narrated as follows.

- The proposed technique operates faster than the existing techniques during close-in faults.
- For the faults involving low resistance and higher magnitude of DC component, the response time of the proposed algorithm is always less than existing methods.
- When fault resistance is higher than the impedance setting of relay, then the existing scheme treats such fault either as the fault of the next zone or out of zone fault. Whereas proposed technique accurately detects low to high resistance fault in its actual zone due to adaptive setting of impedance characteristics and ensures reliable operation.
- Moreover, the proposed scheme is capable to discriminate between zone 1, zone 2 and zone 3 faults and operates with proper time margin provided in it.
- Table I also indicates the fault classified by the modelled fault classifier modules. It shows that each kind of fault is perfectly sensed by the scheme and classification accuracy is 100 %.
- Apart from this, the developed scheme remains stable during load encroachment and saturation of instrument transformers.

Nevertheless, it is observed that for the far end faults, operating time is slightly less in case of wavelet & LDA based technique [14] as compared with proposed algorithm. Also, the operating time is very less in case of conventional DFT, but with increase in DC component and fault resistance there is degradation in their performance. The phase comparison principle based method [4] operates faster during close-in faults but at the same time its response time decreases as fault resistance increases. As the reach setting in the proposed technique is 100 km for zone 1, it does not operate quickly for the out of zone 1 fault, which indicates stability and reliability of the proposed technique. However, in ANFIS based technique [24] due to higher reach setting, the trip signal is generated (Case 30). It can be narrated that the implemented algorithm yields optimum performance parameters in terms of accuracy and response time with adaptive approach.

C. Fault Location Estimation

The outcome of variation in fault location error with respect to actual fault distance from relay location is shown in Fig. 11 for L-G fault applied with $FIA = 0^\circ$ for the different values of fault resistance. The fault locator scheme calculates the location of the fault by taking a ratio of estimated fault impedance to the unit impedance. The actual fault impedance is estimated by using the proposed phasor estimation technique and unit impedance is derived from the knowledge of X/R ratio of transmission line to be protected. Error in the estimation is calculated using eq. (20). It can be observed from the result analysis illustrated in Fig. 11 that the error in fault location estimation is always less than 1 % for wide variation in fault resistance. Thus, compared to existing schemes [10], [12], [13] and [16] in which the optimum error achieved is up to 3 %, the fault location error estimated by proposed method is low for different fault location, fault types and variation in fault resistance.

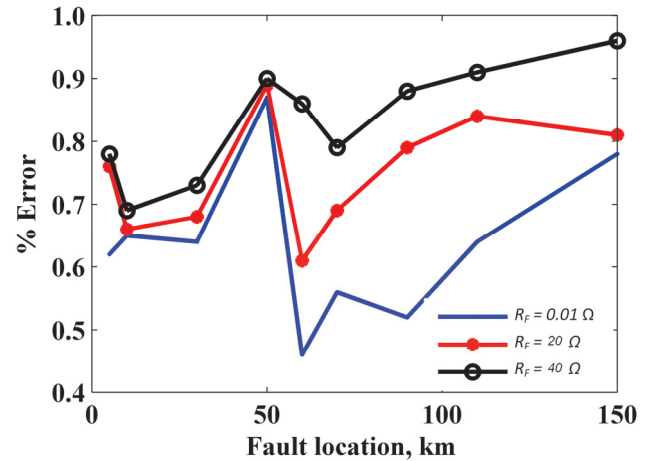


Fig. 11. Percentage of fault location error versus fault distance for L-G fault with $FIA = 0^\circ$.

D. Fault Cases With CT Saturation

The close-in fault imposes severe system disturbances for numerical relaying. When it occurs, fault current will be very high and CTs get saturated depending on the magnitude of current and burden resistance in the secondary side. In this work, CT secondary burden resistance is varied from 5Ω to 20Ω during close-in faults. The proposed scheme is validated for L-G close-in fault applied at 5 km with $FIA = 0^\circ$ and burden resistance of 15Ω . The result for the same is shown in Fig. 12. It is observed that during severe CT saturation the proposed scheme successfully detects the fault in the first zone and generates trip signal within one cycle. This ensures reliability and security of the protection systems.

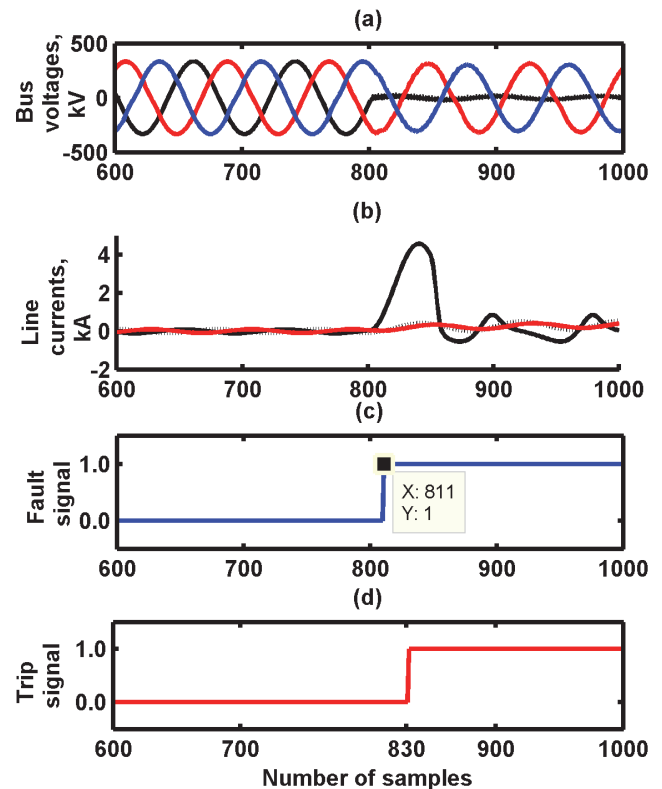


Fig. 12. Wave forms of (a) bus voltages, (b) line currents, (c) fault signal, (d) trip signal during close-in fault at 5 km with $FIA = 0^\circ$ with CT secondary burden of 15Ω .

VI. CONCLUSION

This paper presents novel decision logic to improve the impedance reach of numerical distance relay by adaptive setting of quadrilateral characteristics. The proposed technique implements MFCDF algorithm for fast and accurate phasor estimation of fault impedance followed by slope tracking method for adaptive setting of the numerical relaying. System modeling and simulation is performed in PSCAD software package using multi-run facility for capturing samples of faulty signals during varying power system disturbances and the developed algorithm is validated in MATLAB. The high impedance faults (HIFs) are successfully detected by implementing GDF calculation, slope tracking method and adaptive quadrilateral relay characteristic. The proposed technique is found to be highly precise and faster than the existing methods during close-in fault, high resistance fault, load encroachment, influence of DC component and CT saturation. Fault classifier module is designed for each phase and line to identify the type of fault occurs on transmission line. In order to estimate accurate fault location, a fault locator module is also designed and error in fault location estimation is found within 1 % for each zone of protection. The outcome of the proposed algorithm highlights significant contribution to improve stability and sensitivity of the distance relays. Moreover, the proposed fault identification algorithm can accurately estimate fault instance, fault location and type of fault, which are the desirable attributes of multifunctional numerical relay.

REFERENCES

- [1] Electrical Power Research Institute (EPRI), "Power System Transmission Challenges and Research Needs," California, USA, Nov. 2004.
- [2] Task Force, "U.S. – Canada Power System Outage: Causes & Recommendations", USA, Canada, Apr. 2004.
- [3] "Report on Grid Disturbance in India on 30th July 2012 and Grid Disturbance on 31st July 2012", New Delhi, India, Aug. 2012.
- [4] S. J. Zubić and M. B. Djurić, "A Distance Relay Algorithm Based on Phase Comparison Principle," *Electric Power System Research*, vol. 92, no. 1, pp. 20–28, Nov. 2012. <https://doi.org/10.1016/j.epsr.2012.05.017>
- [5] V. Kale, S. Bhide, and P. Bedekar, "Comparison of Wavelet Transform and Fourier Transform Based Methods of Phasor Estimation for Numerical Relaying," *International Journal of Advances in Engineering Sciences*, vol. 1, no. 1, pp. 55–59, Jan. 2011.
- [6] M. García-Gracia, A. Montañés, N. El Halabi, and M. P. Comech, "High Resistive Zero-Crossing Instant Fault Detection and Location Scheme Based on Wavelet Analysis," *Electric Power Systems Research*, vol. 92, no. 1, pp. 138–144, Nov. 2012. <https://doi.org/10.1016/j.epsr.2012.06.005>
- [7] A. Zamora, M. R. Arrieta Paternina, E. Vazquez-Martinez, and J. M. Ramirez, "Digital Filter for Phasor Estimation Applied to Distance Relays," *IET Generation, Transmission Distribution*, vol. 9, no. 14, pp. 1954–1963, Nov. 2015. <https://doi.org/10.1049/iet-gtd.2014.1220>
- [8] P. Jafarian and M. Sanaye-Pasand, "Weighted Least Error Squares Based Variable Window Phasor Estimator for Distance Relaying Application," *IET Generation Transmission Distribution*, vol. 5, no. 3, pp. 298–306, 2011. <https://doi.org/10.1049/iet-gtd.2010.0244>
- [9] C.-S. Yu, "A Discrete Fourier Transform-Based Adaptive Mimic Phasor Estimator for Distance Relaying Applications," *IEEE Transactions on Power Delivery*, vol. 21, no. 4, pp. 1836–1846, Oct. 2006. <https://doi.org/10.1109/tpwrd.2006.874609>
- [10] N. El Halabi, M. García-Gracia, S. M. Arroyo, and A. Alonso, "Application of Distance Relaying Scheme to Compensate Fault Location Errors," *Electric Power Syst. Research*, vol. 81, no. 1, pp. 1681–1687, Aug. 2011. <https://doi.org/10.1016/j.epsr.2011.04.001>
- [11] J. Linčiks and D. Baranovskis, "Single Phase Earth Fault Location in the Medium Voltage Distribution Networks," *Electrical Control and Communication Engineering*, vol. 25, no. 25, pp. 13–18, May 2010. <https://doi.org/10.2478/v10144-009-0002-6>
- [12] M. Wen, D. Chen, and X. Yin, "A Novel Fast Distance Relay for Long Transmission Line," *Electric Power and Energy Systems*, vol. 63, no. 1, pp. 681–686, Dec. 2014. <https://doi.org/10.1016/j.ijepes.2014.06.058>
- [13] M. Jamil, A. Kalam, A. Q. Ansari, M. Rizwan, "Generalized Neural Network and Wavelet Transform Based Approach for Fault Location Estimation of a Transmission Line," *Applied Soft Computing*, vol. 19, no. 1, pp. 322–332, Jun. 2014. <https://doi.org/10.1016/j.asoc.2014.02.020>
- [14] A. Yadav and A. Swetapadma, "A Novel Transmission Line Relaying Scheme for Fault Detection and Classification Using Wavelet Transform and Linear Discriminant Analysis," *Ain Shams Engineering Journal*, vol. 6, no. 1, pp. 199–209, Mar. 2015. <https://doi.org/10.1016/j.asej.2014.10.005>
- [15] A. Swetapadma and A. Yadav, "Improved Fault Location Algorithm for Multi-Location Faults, Transforming Faults and Shunt Faults in TCSC Compensated Transmission Line," *IET Generation, Transmission Distribution*, vol. 9, no. 13, pp. 1597–1607, Oct. 2015. <https://doi.org/10.1049/iet-gtd.2014.0981>
- [16] N. Roy and K. Bhattacharya, "Detection, Classification and Estimation of Fault Location on an Overhead Transmission Line Using S-Transform and Neural Network," *Electric Power Components and Systems*, vol. 43, no. 1, pp. 461–472, Feb. 2015. <https://doi.org/10.1080/15325008.2014.986776>
- [17] R. G. Stockwell, L. Mansinha, and R. P. Lowe, "Localization of the Complex Spectrum: The S-Transform," *IEEE Transaction on Signal Processing*, vol. 44, no. 4, pp. 998–1001, Apr. 1996. <https://doi.org/10.1109/78.492555>
- [18] S.-L. Yu and J.-C. Gu, "Removal of Decaying DC in Current and Voltage Signals Using a Modified Fourier Filter Algorithm," *IEEE Transactions on Power Delivery*, vol. 16, no. 3, pp. 372–378, Jul. 2001. <https://doi.org/10.1109/61.924813>
- [19] J. Upendar, C. P. Gupta, and G. K. Singh, "Discrete Wavelet Transform and Genetic Algorithm Based Fault Classification of Transmission Systems", in *15th National Power Systems Conference (NPSC)*, Bombay, India, Dec. 2008, pp. 323–328. <https://doi.org/10.1109/indcon.2008.4768827>
- [20] P. Jafarian and M. Sanaye-Pasand, "High Frequency Transient Based Protection of Multi terminal Transmission Lines Using the SVM Technique", *IEEE Transaction on Power Delivery*, vol. 28, no. 1, pp. 188–196, Jan. 2013. <https://doi.org/10.1109/tpwrd.2012.2215925>
- [21] A. Sauhats, A. Utans, G. Pashnin, and D. Antonovs, "Out-of-Step Relays Testing Procedure," *Electrical Control and Communication Engineering*, vol. 28, no. 1, pp. 9–14, Jan. 2011. <https://doi.org/10.2478/v10144-011-0001-2>
- [22] U. J. Patel, N. G. Chothani, and P. J. Bhatt, "Distance Relaying With Power Swing Detection Based on Voltage and Reactive Power Sensitivity," *Emerging Electric Power Systems*, vol. 17, no. 1, pp. 27–38, Jan. 2016. <https://doi.org/10.1515/ijeeps-2015-0109>
- [23] E. Sorrentino, "Comparison of Five Methods of Compensation for Ground Distance Function and Assessment of Their Effect on the Resistive Reach in Quadrilateral Characteristics," *Electric Power & Energy Systems*, vol. 61, no. 1, pp. 440–445, Oct. 2014. <https://doi.org/10.1016/j.ijepes.2014.03.049>
- [24] M. Sanaye-Pasand and P. Jafarian, "An Adaptive Decision Logic to Enhance Distance Protection of Transmission Lines," *IEEE Transaction on Power Delivery*, vol. 26, no. 4, pp. 2134–2144, Oct. 2011. <https://doi.org/10.1109/tpwrd.2011.2159404>
- [25] A. Yadav and A. Swetapadma, "Enhancing the Performance of Transmission Line Directional Relaying, Fault Classification and Fault Location Schemes Using Fuzzy Inference System," *IET Generation, Transmission & Distribution*, vol. 9, no. 6, pp. 580–591, Apr 2015. <https://doi.org/10.1049/iet-gtd.2014.0498>
- [26] Sub-Committee on Relay/Protection Under Task Force for Power System Analysis under Contingencies, "Model Setting Calculations For Typical IEDs Line Protection Setting Guide Lines Protection System Audit Check List Recommendations For Protection Management", New Delhi, 2014, pp. 37–44.



Ujjaval J. Patel graduated from the L.D. College of Engineering, Ahmedabad, in 2001, and received his Master degree from the Faculty of Technology of M. S. University – Vadodara in 2008. Since July 2014, he has pursued the degree of Doctor of Philosophy from Charusat University, Anand. He is currently working as Head of Department of Electrical Engineering at Vadodara Institute of Engineering, Vadodara, India. His special fields of interest include microcontroller based control of real time applications, numerical relaying for power system protection and power quality improvements.

Address: Department of Electrical Engineering, Vadodara Institute of Engineering, At. Kotambi, Vadodara-391510, Gujarat, India.

Email: ujjaval58@rediffmail.com

ORCID iD: <https://orcid.org/0000-0003-2631-4107>



Nilesh G. Chothani graduated from Saurashtra University, Rajkot, Gujarat, in 2001, and received M. E. degrees in power system from Sardar Patel University, Vallabh Vidyanagar, India, in 2004. He received his Ph.D. degree in Electrical Engineering from Sardar Patel University, India, in 2013. Currently, he is working as Head of the Department of Electrical Engineering, ADIT, New Vallabh Vidyanagar, India. He has published more than 35 papers at international and national levels. One of his international conference papers was selected as the best IEEE paper and awarded as

work of excellence. He is also involved in a research project sanctioned by DST, New Delhi, India. His research interests include power system analysis and simulation, system protection, power system stability and artificial intelligence.

Address: Department of Electrical Engineering, A.D. Patel Institute of Technology, New V.V.Nagar, Anand-388121, Gujarat, India.

Email: chothani_nilesh@rediffmail.com

ORCID iD: <https://orcid.org/0000-0002-9936-1687>



Pragnesh J. Bhatt, member of IEEE, received his Ph.D. degree from S. V. National Institute of Technology, Surat, India, in 2012. He is working as Professor and Head of the Department of Electrical Engineering at C. S. Patel Institute of Technology, Charusat, India. His research areas are power system analysis, power system dynamics and stability, grid integration of wind power generation, power system protection and distributed generation.

Address: Department of Electrical Engineering,

C.S. Patel Institute of Technology, Changa, Anand-388421, Gujarat, India.

Email: pragneshbhatt.ee@charusat.ac.in

ORCID iD: <https://orcid.org/0000-0002-0262-9991>